RSC Advances

ROYAL SOCIETY OF CHEMISTRY

www.rsc.org/advances

Graphical Abstract

Conversion of the cyclohexane oxidation reaction with TBHP catalyzed by VTiX in different solvents.

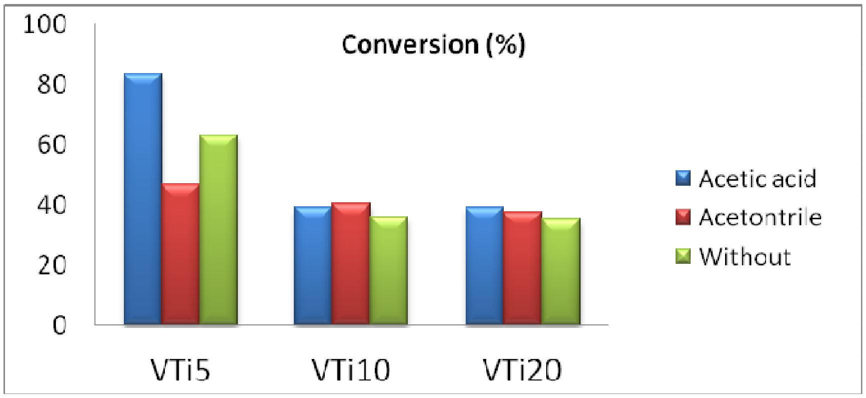

RSC Advances RSCPublishing

ARTICLE

Preparation and characterization of MTiX for the catalytic oxidation of cyclohexane

Cite this: DOI: 10.1039/x0xx00000x

A. Bellifa[a], A. Choukchou-Braham*[b], C. Kappenstein[c] and L. Pirault-Roy[c]

Received 00th March 2014,
Accepted 00th ………….. 2014

DOI: 10.1039/x0xx00000x

www.rsc.org/

MTiX (M = Cr and V) samples, with 0, 5, 10 and 20 of atomic percentage, were synthesised by sol-gel method and calcined at 400 °C under air. The XRD analysis results indicated that the materials presented a crystalline structure with the presence of TiO_2 anatase forms. BET analysis showed that the surface area varied with the variation of metal content. EDX analysis showed a heterogeneous distribution of samples. The results of pyridine adsorption followed by FT-IR indicated that Brønsted and Lewis acid sites are present on the surface of catalysts. Liquid phase oxidation of cyclohexane was carried out under milder reaction conditions over MTiX catalysts using tert-butyl hydroperoxide (TBHP) as oxidant, acetic acid and acetonitrile as solvents. The results indicated that conversion depends on metal content and solvent polarity. Chromium is selective for cyclohexanol. The best result was obtained with VTi20 with 35 % of conversion and 92 % of olone selectivity.

Introduction

Sol–gel procedures are among the most important and versatile methods used for the preparation of inorganic and hybride organic–inorganic materials[1]. The process has been known for 100 years, but in the last 20 years, it has become an attractive and intensive research area for the preparation of glass, ceramics, heterogeneous catalysts and several other highly homogeneous materials. Recently, the sol–gel technique has offered new approaches for the synthesis of porous materials, as well as simple and mixed oxides. Each step of the process can be well and easily controlled and modified in order to obtain a specific product displaying the best catalytic characteristics[2-4].

Transition metals are known for their redox properties and their capacity to catalyse the oxidation of hydrocarbons. Chromium-based catalysts have been widely examined for polymerization, hydrogenation-dehydrogenation, isomerization, aromatization, partial oxidation, and DeNOx reaction because of the peculiar characteristics of chromium oxide species on the surface of the support, including the oxidation state, coordination environment, and degree of polymerization. This versatility of supported chromium oxide catalysts has led to extensive fundamental studies on the parameters controlling the molecular structure of chromium oxide on the catalyst surface. Creation of monomeric species on the surface of anatase (TiO_2) is important for high performance of the DeNOx reaction[5]. However, there have been few studies clearly elucidating the roles of the surface chromate species and the supports in oxidation reactions[6].

Catalysts based on V_2O_5-TiO_2 continue to be a research subject of intense focus, owing to the diversity of catalytic properties, such as those encountered in chemical industry and in air pollution control[7–14]. Vanadium oxide is deposited on different inert surfaces, in order to provide a desirable homogeneous dispersion, mechanical strength as well as thermal stability leading to a continuous catalytic activity, even at elevated temperatures[13,15,16]. Extensive studies have been devoted to such catalysts regarding the dispersion, surface structure, oxidation states and reducibility of supported vanadia species under different conditions; these properties have been correlated with the performance in selective oxidation reactions[13–16].

In the last two decades, considerable applied as well as fundamental research efforts have been made in the activation and functionalization of hydrocarbons. The oxidation of cyclohexane represents a typical example for this type of reactions which have become the theme of several researches these last years[17-23]. The cyclohexanol-cyclohexanone mixture, called "olone", is the main product of the cyclohexane oxidation reaction: 10^6 tonnes of this mixture are yearly produced, and then further converted to adipic acid leading finally to nylon. Currently, in industrial oxidation processes, the conversion of cyclohexane is lower than 3.9 %; however the selectivity of cyclohexanol and cyclohexanone is approximately 78 %[24]. In industrial processes, the aerobic

---

[a] *Laboratoire de Matériaux, Applications et Environnement, Faculté des Sciences et Technologie, Université de Mascara, Algeria.*
[b] *Laboratoire de Catalyse et Synthèse en Chimie Organique, Faculté des Sciences, Université de Tlemcen, Algeria. Email : cba@mail.univ-tlemcen.dz*
[c] *IC2MP UMR-CNRS 7285, Institute of Chemistry of Mediums and Materials of Poitiers, Faculty of Science, 86022 Poitiers, France.*

cyclohexane oxidation is operated at 415–435 K and 1–2 MPa with Mn and Co naphthenates as catalysts.

In spite of the good catalytic activity obtained when using the homogeneous catalysis, the disadvantages of these processes remain in the difficulty and cost to separate the catalyst from the reactional mixture, and the pollution caused by the rejections. Therefore, the development of effective recyclable solid catalysts could offer some advantages. Leaching in the liquid phase can be avoided, provided that anhydrous *tert*-butyl hydroperoxide be used. However, the use of aqueous solutions of H_2O_2 (30 %) or *tert*-butyl hydroperoxide (70 %) will lead to considerable metal leaching [19].

Several studies have been carried out to optimize powerful active and selective catalysts for the oxidation reaction of cyclohexane [25-33]. The modified mixed oxide Sb–V_2O_5/TiO_2 has been used in the oxidative dehydrogenation of propane by Stelzer et al.[34]. A conversion of approximately 25 % has been reported for materials containing 10 wt.% vanadium. The conversion decreases when the vanadium amount decreases. The propene selectivity is about 43 %, whereas for COx it is about 50 %. In the present work, we have also studied cyclohexane oxidation with hydrogen peroxide using 20 wt.% V_2O_5–TiO_2 catalysts, prepared by sol–gel route[35]. The results showed a low conversion. The use of acetic acid as solvent and acetone as initiator presented an approximate 8 % conversion into cyclohexanol, with 76 % selectivity. Recently Pt/oxide (Al_2O_3, TiO_2 and ZrO_2) catalysts have been used for the catalytic oxidation of cyclohexane by tert-butyl hydroperoxide[36]. The results showed the catalytic performance of Pt/Al_2O_3 as being very high in terms of turnover frequency.

In this investigation, MTiX (M = Cr and V) catalyst was synthesized by sol-gel process. XRD, BET, EDX and IR were employed to investigate the structural and textural properties of the catalysts. Then, MTiX was used for the liquid oxidation of cyclohexane under mild conditions. The catalytic activity was carried on by varying the metal content of the as well as the reaction solvent.

Experimental

Synthesis of samples

STARTING MATERIALS

The following chemicals were employed for the preparation of MTiX: Titanium butoxide $Ti(OC_4H_9)_4$ (Aldrich, 97 %), Vanadium (V) oxytripropoxide $OV(OC_3H_7)_3$ (Aldrich, 98 %) and Chromium (III) nitrate nanohydrate $Cr(NO_3)_3x9H_2O$ (Aldrich, 99 %).

The following chemicals were used for catalytic reactions: Tertiobutyl-hydroperoxide TBHP (Aldrich, 70 wt.% in water), Cyclohexane (Prolabo, 98 %).

SYNTHESIS PROCEDURE

The samples were synthetized by sol-gel method[37]. The preparation of TiO_2 was carried out in a 100 mL beaker. Titanium butoxide was dissolved in absolute ethanol. The mixture was stirred for 30 min and then a solution of ethanol and nitric acid was added dropwise in the mixture. The white gel obtained was dried in a sand bath at 60 °C for 6 h, then in an oven at 120 °C for a night. Next, the sample was calcined in a muffle furnace at 400 °C for 4 h, under air atmosphere.

The samples of MTiX were prepared in the same way as that adopted for TiO_2, with the addition of an aqueous solution of chromium nitrate or vanadium (V) oxytripropoxide before adding the nitric acid solution to get the final metal contents of 5, 10 and 20 %.The samples were called MTi5, MTi10 and MTi20 for 5, 10 and 20 of atomic percent, respectively.

Catalyst characterization

Micrometrics Tristar 3000 instrument was used to measure the adsorption-desorption isotherms at liquid nitrogen temperature (77 K) to determine the specific area and calculate the mean pore size using BJH methods. The samples were outgassed at 363 K for 1 h then at 623 K for 10 h under a flow of 30 % nitrogen in helium.

The crystalline phases of the samples were identified by X-ray powder diffraction (XRD) using Bruker D8-ADVANTED and D5005 diffractometers with Cu Kα radiation (λKα1 = 0.15406 nm). The diffractograms were obtained under the following conditions: dwell time: 2 s; step: 0.04 ° 2θ; divergence slit: 0.3 °. The crystalline phases were identified by comparison with Powder Diffraction Files (PDF) standards from ICDD.

To characterize the physical and chemical alterations of doped TiO_2 materials, thermo gravimetric analysis (TGA) and differential thermal analysis (DTA) were performed on calcined powders (15 to 30 mg), from room temperature to 1000 °C, using a Thermal Analyst STD 2960 TA Instrument. The samples were heated at a rate of 10 °C min^{-1} for measurements under dry air flow.

The acidity of samples was characterized by pyridine adsorption followed by IR spectroscopy. The IR spectra were recorded on Nicolet Magna IR spectrometer using a thin wafer (16 mm in diameter, 10-15 $mg.cm^{-2}$) activated *in situ* in the IR cell under secondary vacuum (10^{-3} Pa) at 200 °C for 2 h. Pyridine was adsorbed on the samples at 150 °C. The IR spectra were recorded at room temperature after activation, and pyridine thermo desorption under vacuum (10^{-3} Pa) for 1 h at 150 °C. The total amounts of Lewis and Brønsted acid sites accessible to pyridine were quantified by estimating the difference between P_{150} (spectrum of catalyst after pyridine adsorption/desorption) and P_{ref} (spectrum of catalyst before pyridine adsorption).

Catalytic reactions

First, TBHP was stirred with cyclohexane in order to perform a phase transfer from water to cyclohexane. In a typical reaction, 64 mmol of cyclohexane and 64 mmol of TBHP as oxidant were mixed in a closed Erlenmeyer flask and magnetically stirred for 24 h. The organic phase was then separated from the aqueous phase.

Cyclohexane oxidation reactions were carried out in a 250 mL three-necked flask, placed in a temperature equilibrated oil bath and fitted with a reflux condenser. The solvent (40 mL) was added to the TBHP-cyclohexane mixture. At 70 °C, a quantity of 30 mg of catalyst (MTiX) was subsequently added to the reaction mixture (time zero). The products were analyzed by gas chromatography (GC), taking aliquots (0.5 µL) at different reaction times. A Varian CP-3800 gas chromatograph equipped with a CP-WAX 52 CB column and a flame ionization detector (FID) were used. Before GC analysis, the remaining TBHP was decomposed by introducing an excess of triphenylphosphine.

Results and discussion

Characterization

The N_2 adsorption-desorption isotherms of the different samples are reported in Fig. 1. The isotherm profile for all samples corresponds to a type IV with the presence of a hysteresis loop indicating the existence of mesopores in the samples. A sharp increase in the adsorption volume of N_2 was observed in the P/P_0 range of 0.4-0.8 and can be attributed to the capillary condensation, indicating a good homogeneity of the samples. The values of the specific surface, pore volume and pore size are shown in Table 1. The specific surface area increases with increasing content of metal from 5 to 10 %. MTi20 have small specific surface area than MTi10.

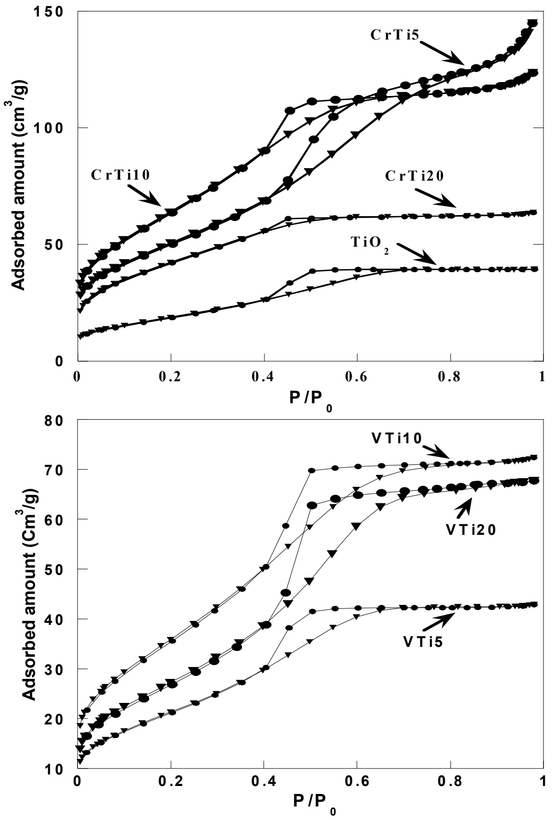

Fig.1 Isotherms for adsorption of nitrogen on MTiX samples

IR spectra of pyridine adsorption (Fig. 2 and Fig. 3) show the presence of Lewis acid sites (1455 cm^{-1}) in all samples. MTi5 displays the highest Lewis acid quantity. We note the presence of Brønsted acid sites (1545 cm^{-1} and 1637 cm^{-1}) only for CrTi20 (Table 1) (cf. ESI; Fig. S1†). As the metal content decreases, the number of Lewis acid sites goes down while that of Brønsted acid sites rises[38].

Table 1 Surface area, porous volume, pore size and acidity of MTiX samples

Sample	S_{BET} ($m^2.g^{-1}$)	Pore volume ($cm^3.g^{-1}$)	Average pore size (nm)	L.A (µmol.g^{-1})	B.A (µmol.g^{-1})
TiO_2	68	0.06	3.6	197	0
CrTi5	180	0.22	5.0	239	0
CrTi10	230	0.19	3.3	28	0
CrTi20	152	0.10	2.6	16	74
VTi5	76	0.07	3.5	177	0
VTi10	129	0.11	3.5	/	/
VTi20	98	0.10	4.0	23	0

Samples calcined at 400°C; B.A: Brønsted Acidity; L.A: Lewis Acidity

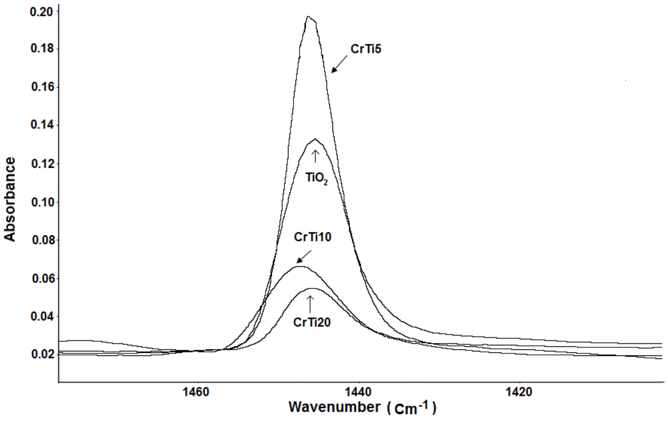

Fig. 2 IR adsorption spectrum of pyridine for CrtiX; evacuation at 150°C.

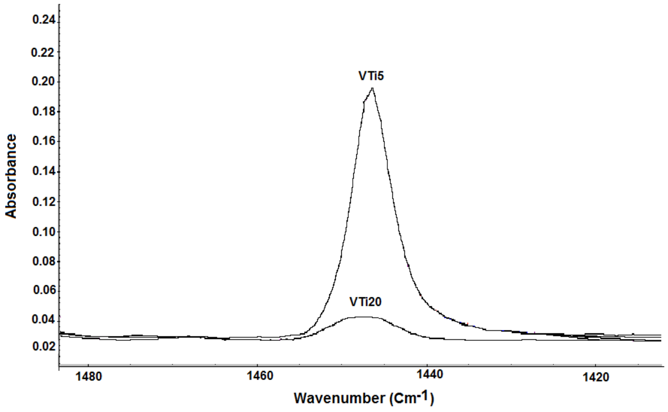

Fig. 3 IR adsorption spectrum of pyridine for VTiX; evacuation at 150 °C.

X-ray diffraction (XRD) patterns of the samples calcined at 400°C are shown in Fig. 4. The XRD patterns of the samples show the crystalline structure of pure anatase phase. No corresponding peaks to rutile, brookite, chromium and vanadium phase were observed. The peak at 44° of 2θ is attributed to Kanthal phase.

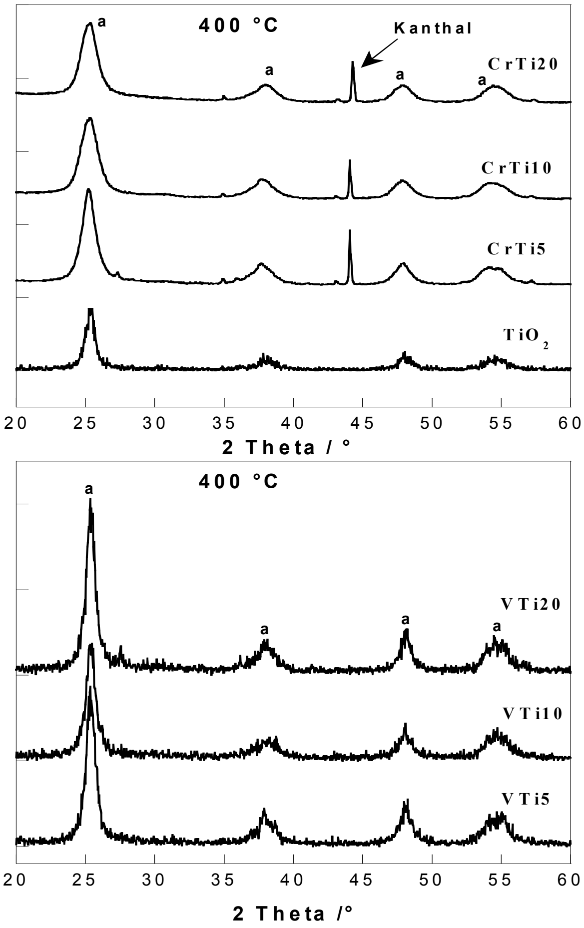

Fig. 4 X-ray diffraction (XRD) patterns of MTiX; a: anatase

For the samples calcined at 400 °C, the curves of TGA-TDA analysis (cf. ESI; Fig. S2† and S3†) display one endothermic peak in the range 0 - 200 °C, corresponding to desorption of water previously adsorbed on the surface, with a weight loss between 5 and 7 %. In the range of 0 - 400 °C, a mass loss of 3.6 %, 9-11 % and 3-4 % was found for TiO_2, CrTiX and VTiX, respectively. On the other hand, the total weight loss observed between 400 °C and 800 °C was less than 1% for VTiX and 0.6, 0.94 and 1.45 % for CrTi5, CrTi10 and CrTi20, respectively. This last result can be attributed to the presence of residual hydroxyl groups due to the increase of metal content which can be removed by a temperature increase[39]. No exothermic peak was observed, and this characterizes the anatase to rutile transition.

EDX analysis, focusing on different zones of the sample CrTi20 (Fig. 5), shows four emission peaks, two for titanium (around 4500 eV and 5000 eV) and two for chromium (around 5400 eV and 6000 eV). In this work, we present the EDX of one zone only for the CrTi20 sample. The content ratio between titanium and chromium in various zones is evaluated from their relative intensities (Table 2). The results showed that the ratio is almost the same for the three zones. As a conclusion, EDX analysis evidenced a homogeneous distribution of titanium and chromium in the sample of CrTi20.

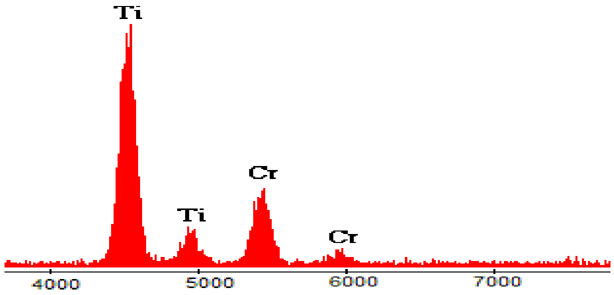

Fig. 5 EDX analysis of zone 3 of the CrTi20 sample.

Table 2 Percentage of Ti and Cr, calculated from their intensities in CrTi20

Zone	1	2	3
%Ti	73	77	76
%Cr	27	23	24
Ti/Cr	2.7	3.3	3.1

For VTi20, the EDX analysis shows that the most intense vanadium emission peak, at about 5000 eV, superimposes a titanium peak (Fig. 6). Nevertheless, the relative intensity of this peak, as compared to that of pure titanium emission at 4500 eV, is not constant. Indeed, for the three zones, the ratio between vanadium and titanium peak intensities is not constant. This last result leads to a heterogeneous distribution of titanium and vanadium in the VTi20 sample.

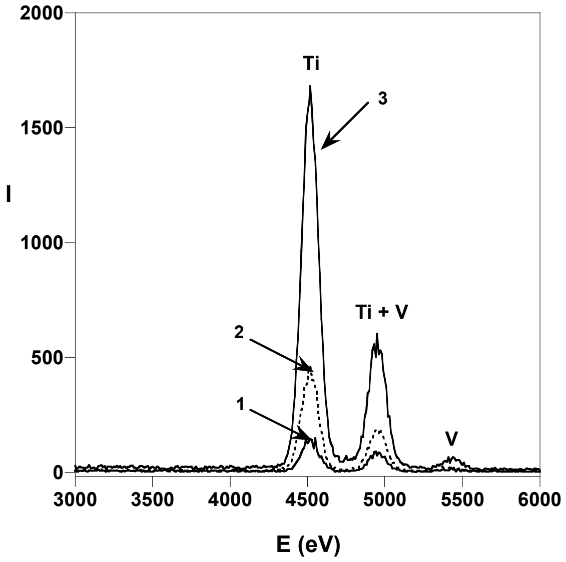

Fig. 6 EDX analysis of different zones of the VTi20 sample.

Catalytic tests

Kinetic studies of the catalytic oxidation of cyclohexane were performed on MTiX samples. The desired products are cyclohexanol and cyclohexanone, but other products did also form[40, 41]. For this study, we focused on the selectivity towards olone only (cyclohexanol + cyclohexanone). Two parameters have been followed during the catalytic oxidation of cyclohexane by TBHP, namely the nature of solvent and the metal content. Cyclohexane was first used as reagent and solvent, but no conversion was noticed for the control reaction after the addition of TBHP, in complete absence of the catalyst. In the presence of TiO_2 alone, using acetonitrile as solvent, a conversion of about 10 % with a selectivity to cyclohexanol of about 03 % were found. No formation of cyclohexnone was obtained.

The results of cyclohexane oxidation are shown in Tables 3 and 4. Cyclohexanol and traces of cyclohexanone were observed, with CrTiX as catalysts. However, a mixture of cyclohexanol and cyclohexanone (olone) was formed with VTiX as catalysts. The ol/one ratio as larger than 1 for all samples, and therefore the cyclohexanol produced was not totally transformed into cyclohexanone. The olone quantity was higher with VTiX than with CrTiX.

Table 3 Cyclohexane oxidation with MTiX

	Without		*Acetonitrile*		*Acetic acid*	
Catalyst	*Cy-ol (mmol)*	*Cy-one (mmol)*	*Cy-ol (mmol)*	*Cy-one mmol)*	*Cy-ol (mmol)*	*Cy-one (mmol)*
CrTi5	4.84	0.00	2.87	0.00	5.47	0.23
CrTi10	5.80	0.00	3.55	0.00	4.91	0.00
CrTi20	5.52	0.00	4.04	0.70	4.86	0.50
VTi5	8.17	4.65	3.20	3.81	7.26	4.70
VTi10	2.95	1.80	2.37	0.87	3.70	2.84
VTi20	11.86	8.73	3.67	0.92	4.22	3.46

C_6H_{12} (64 mmol), TBHP (64 mmol), T = 70°C, t = 6 h; Cy-ol :cyclohexanol ; Cy-one :cyclohexanone

Table 4 Variation of conversion and olone selectivity

	Without		*Acetonitrile*		*Acetic acid*	
Catalyst	*Conv. (%)*	*olone (%)*	*Conv. (%)*	*olone (%)*	*Conv. (%)*	*olone (%)*
CrTi5	20.1	37.8	41.3	11.6	51.2	17.4
CrTi10	42.9	21.1	45.4	13.1	46.2	16.6
CrTi20	44.3	19.5	64.3	12.3	21.6	38.8
VTi5	62.8	31.9	46.7	25.1	83.1	22.5
VTi10	35.8	20.8	40.3	13.4	38.9	26.3
VTi20	34.9	92.1	37.5	20.5	38.8	31.1

C_6H_{12} (64 mmol), TBHP (64 mmol), T = 70 °C, t = 6 h ; Conv. : Conversion

The best olone quantity was obtained without solvent. The olone selectivity decreased when the chromium content increased from 5 to 20 %, whereas an excess of vanadium content led to higher olone selectivity. However, the conversion increased with increases in chromium content and decreased when vanadium content increased.

In the presence of acetonitrile, it is clear that the olone selectivity remains constant for both CrTiX and VTiX. On the other hand, the conversion increased as chromium content increased, whereas it decreased with increasing vanadium content. In our previous study, we found a low conversion when using VTi20 with H_2O_2 as oxidant[35].

When using acetic acid as solvent, the olone selectivity increases while the metal content increases, whereas the conversion decreases with increasing metal content.

The catalytic activity of CrTiX is not correlated to the specific surface but is directly related to the amount of chromium present. Conversion is in good correlation with the increase in chromium content, except in the case of acetic acid as solvent. On the other hand, the variation of conversion depends on the reaction medium. Catalytic activity is enhanced in the presence of a polar solvent. Therefore conversion varies in the following order: acetonitrile > acetic acid > cyclohexane (without solvent).

In the case of VTiX, conversion remains constant with high vanadium content and is favored for small quantities. We found that the best conversion is obtained with acetic acid as solvent. Indeed, the conversion varies in the following order: acetic acid > cyclohexane ≥ acetonitrile. In general, VTiX samples are more active than those of CrTiX. The best conversion (83 %) is obtained with VTi5 in presence of acetic acid as solvent, and the best olone selectivity (92 %) is obtained with VTi20, without solvent. The best catalyst is VTi20 with 35 % of conversion and 92 % of olone selectivity.

The reactivity of the catalysts in liquid phase oxidation reactions depends on the polarity, the protic/aprotic character of the solvent and the hydrophobic/hydrophilic nature of the catalyst associated with the nature of the oxidant. This is such a complex mixture that it is difficult to give a reliable explanation. We note that if acetic acid is used as solvent, per acid is formed; it enables a better reactivity, as already obtained for the conversion values of MTi5. We can also explain our results by a competition between the adsorption of reactants and desorption of products. In the case of VTi20, we have good "olone" selectivity in the free solvent because the products formed are easily desorbed.

Conclusions

The catalyst MTiX (M = Cr and V; X = 0, 5, 10 and 20 %) was prepared by the sol–gel method and calcined at 400 °C. XRD analysis showed that materials present a crystalline structure with the presence of TiO_2 anatase phase. The specific surface of samples increased with the metal content but decreased for an excessive content. The EDX analysis evidenced a heterogeneous distribution of titanium and vanadium in the VTi20 sample. However, a homogeneous distribution of titanium and chromium has been reported in the CrTi20 sample. Regarding cyclohexane oxidation, the results showed that all catalysts were active, with and without solvent. The presence of chromium leads to the formation of cyclohexanol only, whereas the cyclohexanol-cyclohexanone mixture is produced in presence of vanadium. The samples are more active and selective with the presence of vanadium than with chromium. Conversion variation and olone selectivity cannot be correlated with the specific surface variation and acidity. However, the activity of catalysts does depend on the metal content and the nature of solvent.

Acknowledgements

Authors thank the Algerian Ministry of Higher Education and Scientific Research for the fellowship funding in the University of Poitiers, France.

Notes and references

† Electronic supplementary information (ESI) available. See DOI: 10.1039

1 A. Baiker, *Stud. Surf. Sci. Catal.*, 1996, **101**, 51.
2 Q. Xiao, Y.Liu, Y. Zhong, W.Zhu, *J. Mater. Chem.,* 2011, **21**, 3838.
3 H.S. Chen, RV. Kumar, *RSC Advances,* 2012, **2**, 2294.
4 Z. Su, K. Sun, Z. Han, H. Cui, F. Liu, Y. Lai, J. Li, X. Hao, Y. Liu, M. Green, *J. Mater. Chem. A*, 2014, **2**, 500.
5 C.H. Fountzoula, HK. Matralis, C.H. Papadopoulou, G.A. Voyiatzis, CH. Kordulis, *J. Catal.*, 1997, **172**, 391.
6 S.D. Yim, KH. Chang, DJ. Koh, IS. Nam, YG. Kim, *Catal. Today.*, 2000, **63**, 215.
7 D.A. Bulushev, L. Kiwi-Minsker, VI ; Zaikovskii, A. Renken, *J. Catal.*, 2000, **193,** 145.
8 D. Heinz, W.F. Hoelderich, S. Krill, W. Boeck, K. Huthmacher, *J. Catal.*, 2000, **192**, 1.
9 D. Heinz, W. Hoelderich, S. Krill, W. Boeck, K. Huthmacher, *Patent No. EP984005-A*, 2001.
10 X. Zhang, X. Li, J. Wu, R. Yang, Z. Zhang, *Catal. Lett.*, 2009, **130**, 253.
11 Y. Liu, ZB. Wei, ZC. Feng, MF. Luo, P.L. Ying, C. Li, *J. Catal.*, 2001, **202**, 200.
12 H.Y. Chang, SP. Wang, JR. Chang, HS. Sheu, SG. Shyu, *Appl. Catal. B Environ.*, 2012, **111**, 476.
13 D.P. Debecker, K. Bouchmella, R. Delaigle, P. Eloy, C. Poleunis, P. Bertrand, EM. Gaigneaux, PH. Mutin, *Appl. Catal. B Environ.*, 2010, **94**, 38.
14 H. Zhao, S. Bennici, J. Shen, A. Auroux, *Appl. Catal. A Gen.*, 2009, **356**, 121.
15 Y. Sakurai, T. Suzaki, K. Nakagawa, N. Ikenaga, H. Aota, T. Suzuki, *J. Catal.*, 2002, **209**, 16.
16 E. Santacesaria, A. Sorrentino, R. Tesser, M. Di Serio, A. Ruggiero, *J. Mol. Catal. A Chem.*, 2003, **204**, 617.
17 C.-C. Guo, M.-F. Chu, Q. Liu, Y. Liu, D.-C. Guo, X.-Q. Liu, *Appl. Catal. A: Gen.* 2003, 246, 303.
18 M. P. de Almeida, L. Martins, S. Carabineiro, T. Lauterbach, F. Rominger, A. Hashmi, J. Pombeiro, J. Figueiredo, *Catal. Sci. Technol.*, 2013, **3**, 3056.
19 U. Schuchardt, D. Cardoso, R. Sercheli, R. Pereira, RS. Cruz, MC. Guerreiro, D. Mandelli, EV. Spinacé, EL. Pires, *Appl. Catal. A Gen.*, 2001, **211**, 1.
20 S. Shylesh, PP. Samuel, AP. Singh, *Appl. Catal. A Gen.*, 2007, **318**, 128.
21 S. Shylesh, C. Srilakshmi, A.P. Singh, B.G. Anderson, *Microporous Mesoporous Mater*, 2007, **99**, 334.
22 J.Y. Wang, FY. Zhao, RG. Liu, YQ. Hu, *J. Mol. Catal. A Chem.*, 2008, **279**, 153.
23 A. Ebadi, N. Safari, MH. Peyrovi, *Appl. Catal. A Gen.*, 2007, **321**, 135.
24 D.D. Davis, in: W. Gerhartz, S.Y. Yamamoto, T.F. Campbell, R. Pfefferkorn, J.F. Rounsaville (Eds.), 5th ed., Ullmann's *Encyclopedia of Industrial Chemistry*, vol. A1, VCH Publishers, Weinheim, 1985, pp. 269–278.
25 C. Wang, L. Chen, Z. Qi, *Catal. Sci. Technol.*, 2013, **3**, 1123.
26 Y. Cao, X. Luo, H. Yu, F. Peng, H. Wang, G. Ning, *Catal. Sci. Technol.*, 2013, **3**, 2654.
27 P. Wu, Z. Xiong, KP. Loh, XS. Zhao, *Catal. Sci. Technol.*, 2011, **1**, 285.
28 Y. Shiraishi, Y. Sugano, S. Ichikawa, T. Hirai, *Catal. Sci. Technol.*, 2012, **2**, 400.
29 H. Einaga, S. Futamura, T. Ibusuki, *Appl. Catal. B Environ*, 2002, **38**, 215
30 R.S. Cruz, MM. Dauch, U. Schuchardt, R. Kumar, *Stud. Surf. Sci. Catal.*, 2000, **130**, 1037.
31 E.L. Pires, U. Arnold, U. Schuchardt, *J. Mol. Catal. A Chem.*, 2001, **169**, 157.
32 R.S. da Cruz, JMS. Silva, U. Arnold, U. Schuchardt, *J. Mol. Catal. A Chem.*, 2001, **171**, 251.
33 R.S. da Cruz, JMS. Silva, U. Arnold, MS. Sercheli, Schuchardt, *J. Chem. Soc.*, 2002, **13**, 170.
34 J.B. Stelzer, J. Caro, M. Fait, *Catal. Commun.,* 2005, **6**, 1.
35 A. Bellifa, D. Lahcene, YN. Tchenar, A. Choukchou-Braham, R. Bachir, S. Bedrane, C. Kappenstein, *Appl. Catal. A Gen.*, 2006, **305**, 1.
36 I. Hammoumraoui, A. Choukchou-Braham, L. Pirault-Roy, C. Kappenstein, *Bull. Mater. Sci.*, 2011, **34**, 1127.
37 K.R. Zhu, MS. Zhang, J.M. Hong, Z. Yin, *Mater. Sci. Eng. A*, 2005, **403**, 87.
38 T. Onfroy, G. Clet, S.B. Bukallah, T. Visser, M. Houalla, *Appl. Catal. A Gen.*, 2006, **298**, 80.
39 J. Li, Q. Li, Y. Yand, Y. Hao, *J. Alloy. Compd.*, 2011, **509**, 5532.
40 R. Kumar, S. Sithambarama, SL. Suib, *J. Catal.*, 2009, **262**, 304.
41 L. Zhou, J. Xu, H. Miau, F. Wang, X. Li, *Appl. Cata. A Gen.*, 2005, **292**, 223.